

Using the hydrolysis of anhydrides to control gel properties and homogeneity in pH-triggered gelation

Emily R. Draper,^a Laura L. E. Mears,^a Ana M. Castilla,^a Stephen M. King,^b Tom O. McDonald,^a Riaz Akhtar^{c*} and Dave J. Adams^{a*}

^a *Department of Chemistry, University of Liverpool, Crown Street,*

Liverpool, L69 7ZD, UK. E-mail: d.j.adams@liverpool.ac.uk

^b *ISIS Facility, Rutherford Appleton Laboratory, Science and Technology Facilities Council, Didcot, Oxfordshire OX11 0QX, U.K.*

^c *Centre for Materials and Structures, School of Engineering, University of Liverpool, Liverpool L69 3GH, U.K. Email: r.akhtar@liverpool.ac.uk*

SUPPORTING INFORMATION

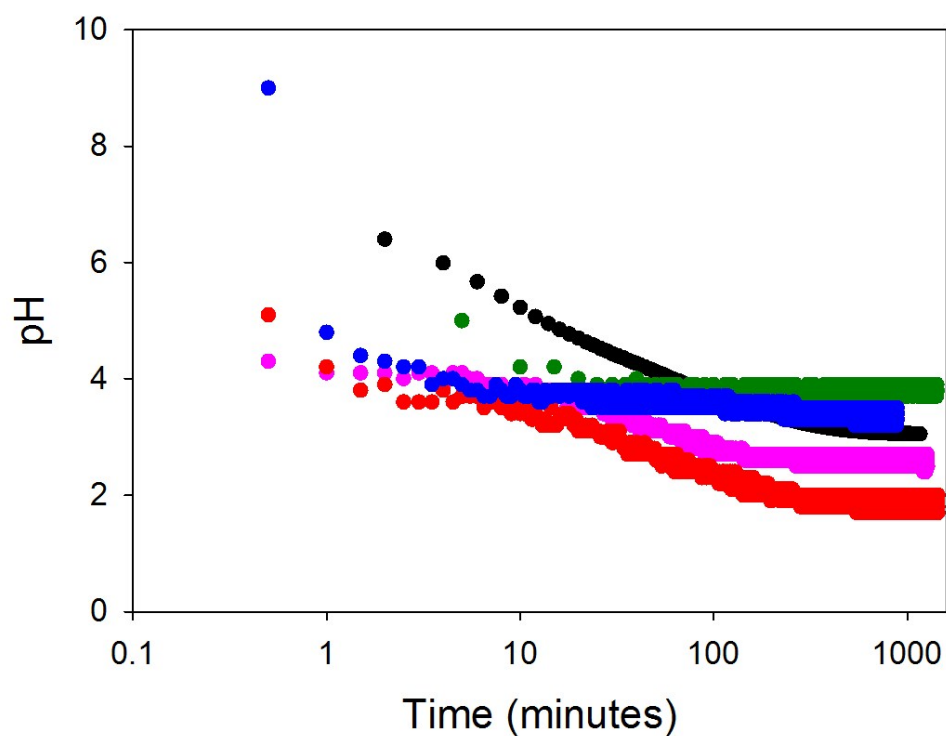


Figure S1. Change in pH during gelation of **1** using different pH triggers (3 molar equivalents with respect to **1**). Blue is for the acetic anhydride data, red is for maleic anhydride, green is for glutaric anhydride, pink is for diglycolic anhydride and black is for GdL.

Molar equivs	Acetic Anhydride	Maleic Anhydride	Glutaric Anhydride	Diglycolic Anhydride	GdL	HCl
1	4.17	3.04	4.24	3.31	4.10	4.62
3	3.89	2.03	2.84	2.67	3.44	4.32
5	3.18	1.76	2.58	2.35	3.18	3.07

Table S1. Final pH values obtained after 18 hours for each of the triggers added to a solution of **1** initially at pH 11.3 at 1, 3, and 5 molar equivalents compared to **1**.

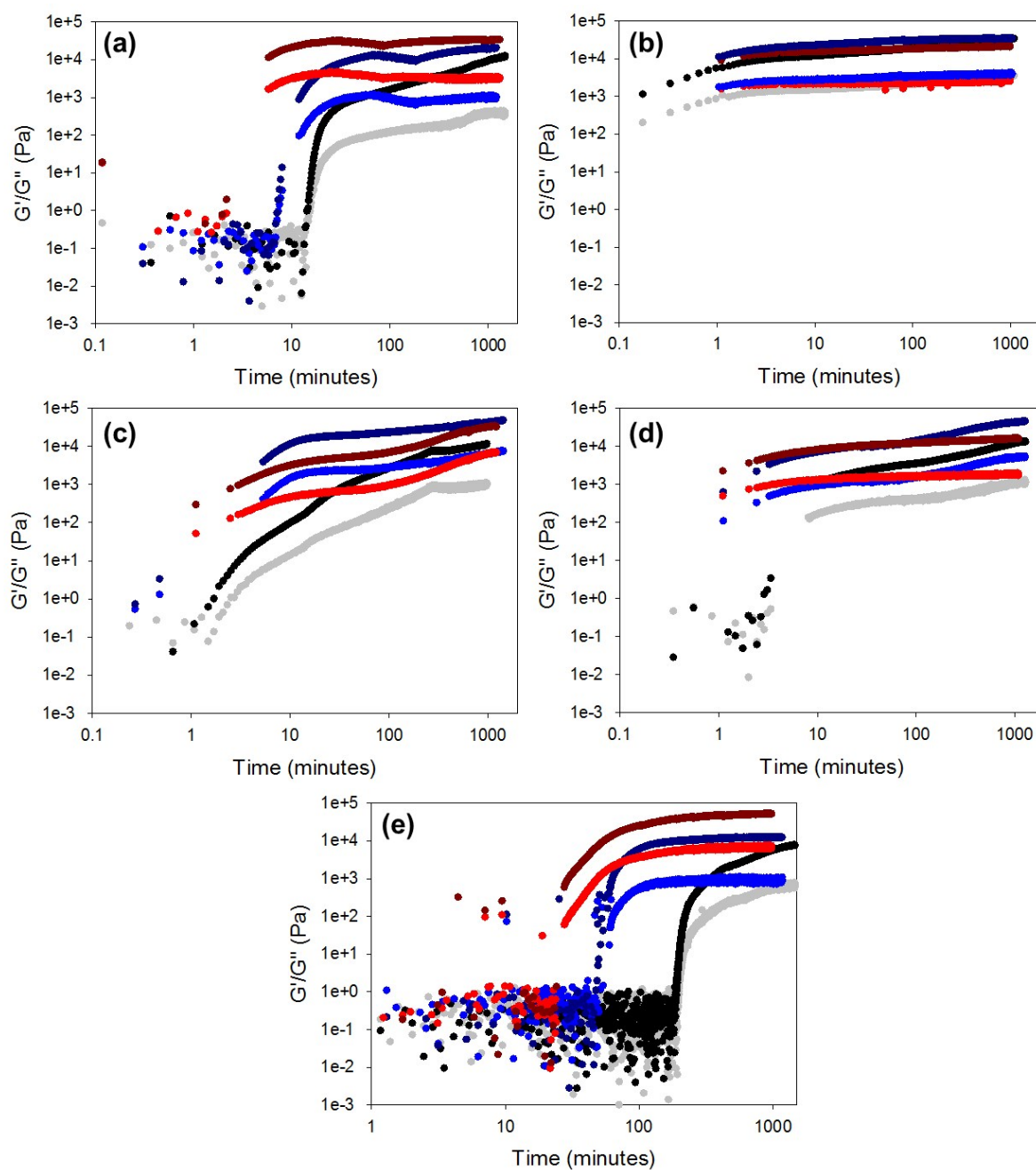


Figure S2. Gelation kinetics of **1** over time using 1 molar equivalent (black and grey), 3 molar equivalents (dark blue and blue) and 5 molar equivalents (dark red and red) of different pH triggers relative to **1**. All data were collected at 25 °C. Dark red, dark blue and black represent G' and grey blue and red represent G'' . (a) is acetic anhydride, (b) is maleic anhydride, (c) is glutaric anhydride (d) is diglycolic anhydride and (e) is GdL. Measurements were recorded at a strain of 0.5 % and at a frequency of 10 rad/s.

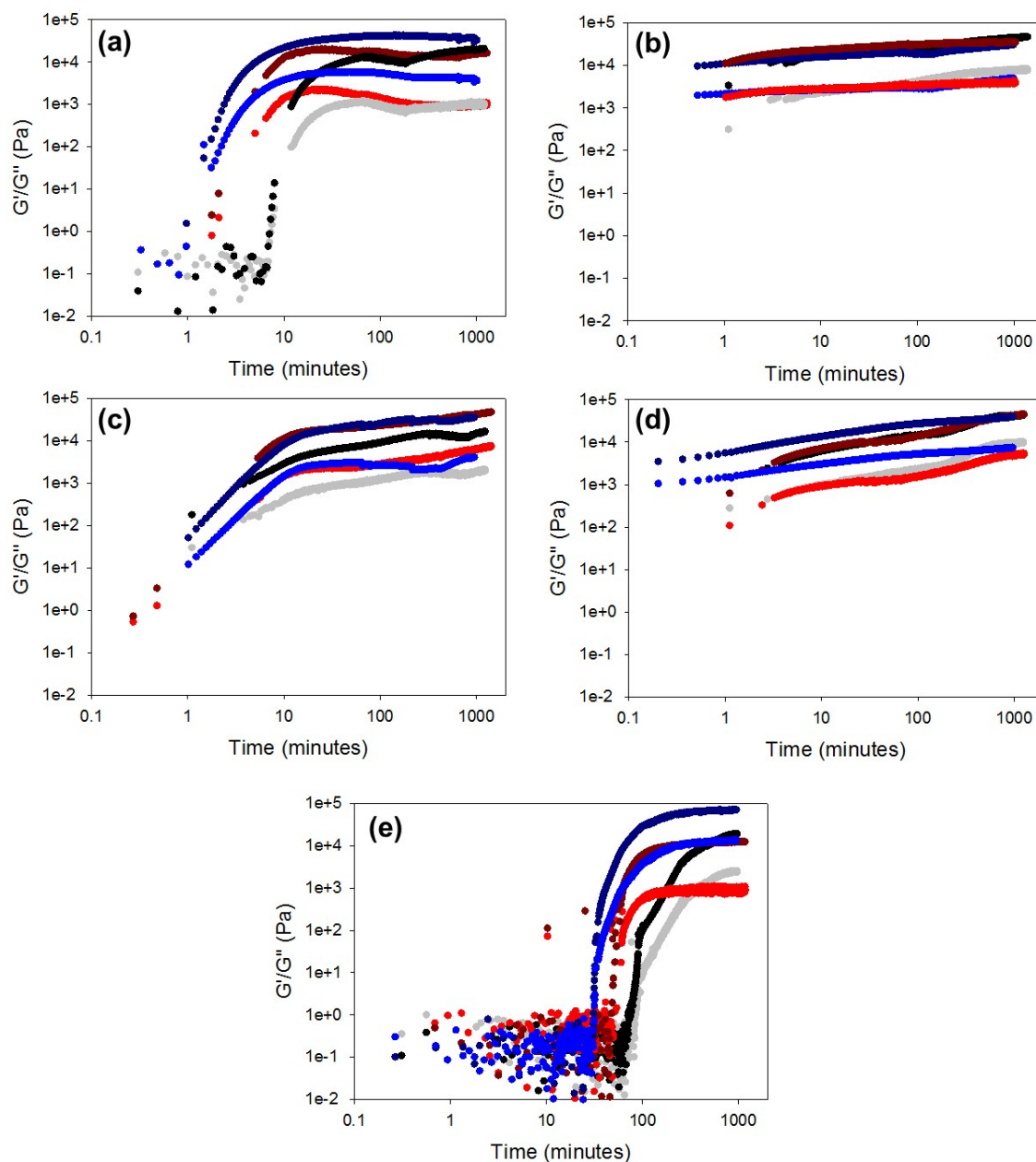


Figure S3. Gelation kinetics of **1** over time using different temperatures: 20 °C (black and grey), at 25 °C (dark blue and blue) and 30 °C (dark red and red) of different pH triggers (3 molar equivalents with respect to **1**). Dark red, dark blue and black represent G' and grey blue and red represent G'' . (a) is acetic anhydride, (b) is maleic anhydride, (c) is glutaric anhydride (d) is diglycolic anhydride and (e) is GdL. Measurements were recorded at a strain of 0.5 % and at a frequency of 10 rad/s.

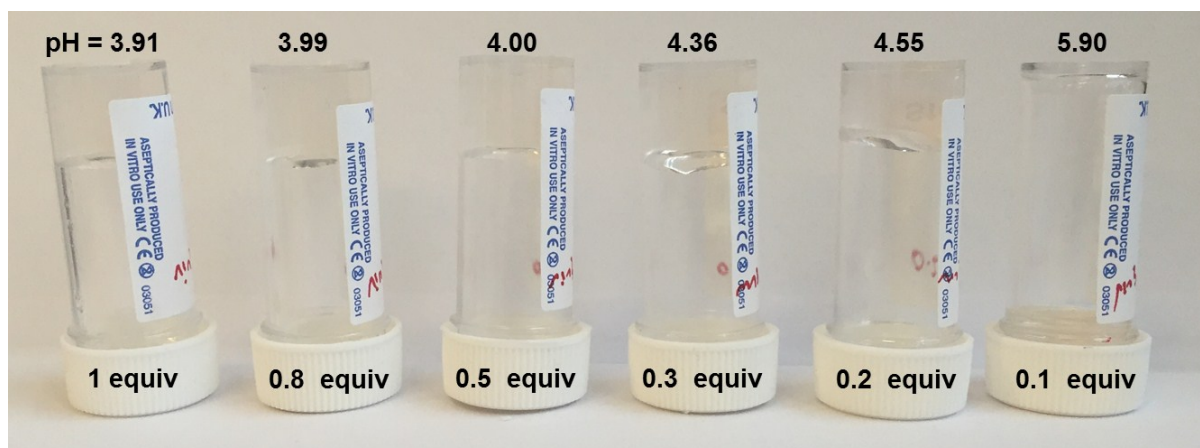


Figure S4. Photographs of samples where different amounts of acetic anhydride have been added to a stock solution of **1**. Gelation only occurs when sufficient anhydride has been added to lower the pH below the pK_a of **1**.

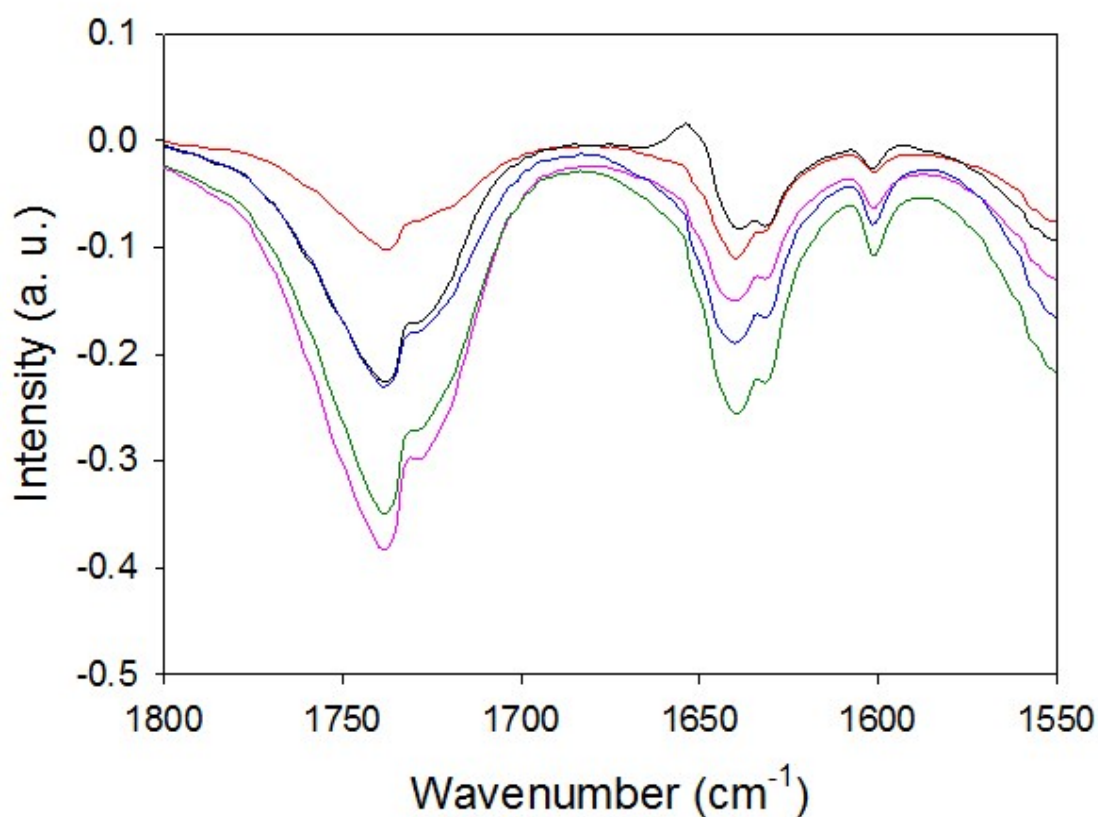


Figure S5. FTIR spectra of gels (3 molar equivalents of each trigger added with respect to **1**) with the background subtracted showing the amide I region. Blue is acetic anhydride, red is maleic anhydride, glutaric anhydride is green, diglycolic anhydride is pink and GdL is black.

SANS model fitting

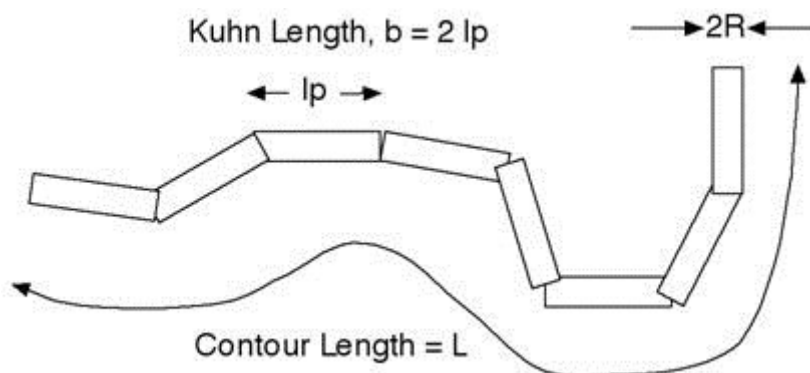


Figure S6. Schematic showing the parameters associated with the dimensions of the worm-like chain in the Kratky-Porod flexible cylinder model within SasView.¹

The model used to fit the SANS data was the Kratky-Porod (KP) flexible cylinder model combined with a power law, Equation 1^{2,3}

$$I = SF_O (SF_{PL} P(Q)_{PL} + SF_{KP} P(Q)_{KP}) + \text{Background} \quad [1]$$

where $P(Q)$ is the relevant scattering function. For $P(Q)_{KP}$ this comprises the product of two terms: one describing the flexible chain with excluded volume (Equation 26 in Reference 2, Supporting Information) and the other describing the cross-section of a rigid rod (Equation 4 in Reference 3, Supporting Information). The flexible cylinder model describes a worm-like chain of length, L , made from freely jointed units with a segment length, lp , which is half of the Kuhn length fitting parameter and a cross-sectional radius, R (Fig. S5). The other parameters in the model include: an overall scale factor, SF_O , fixed at 1; a simple numerical scaling factor for the power law component of the model, SF_{PL} , related to the density of the network; a scale factor for the worm-like chain, SF_{KP} , corresponding to the volume fraction of the cylinders (of the size described by the model); a flat background to account for the incoherent background scattering from the sample; and, in most cases, a polydispersity parameter is also included, this applies a Gaussian distribution to the cross-sectional radius of the of the cylinder.

We have previously fitted data using the Kholodenko-Dirac (KD) worm-like chain model⁴ and in the region we are working the differences between the KD worm and the KP worm, as applied by the flexible chain, are smaller than the uncertainties. The flexible chain model was used here for computational convenience, but both are designed to interpolate between the expected Q^{-1} dependence for the rod-like character of the cylindrical elements, the Q^{-2} associated with the cross-section of the cylinder and a limiting Q^{-4} associated with the globular nature over large distances. A comparison between the model fit obtained from the flexible cylinder model and that of a regular cylinder (both with the additional power law component) is shown in Fig. S6. This demonstrates how the features of the data are not captured by the simpler model.

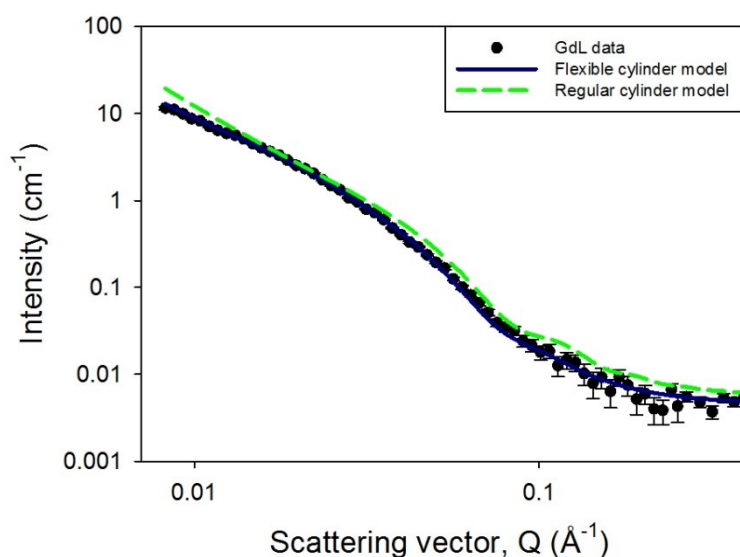


Figure S7. SANS intensity profile for a gel formed using GdL (3 molar equivalents with respect to **1**) formed in 2 mm quartz cuvettes. The solid line represents the model fit generated by the flexible cylinder model and the dashed line shows the model fit using a regular cylinder model.

When fitting, some conditions were imposed such as the Kuhn length had to be larger than $2R$, and less than the overall length. The scattering length densities (SLDs) of the cylinder, made from **1** ($2.5 \pm 0.5 \times 10^{-6} \text{ \AA}^{-2}$), and the solvent, predominantly D_2O ($6.3 \times 10^{-6} \text{ \AA}^{-2}$), were fixed. The slightly higher than theoretical value for the cylinder ($1.54 \times 10^{-6} \text{ \AA}^{-2}$ for a bulk density of 1 g cm^{-3}) is to account for some hydration. This value is correlated with the SF_w parameter, but was kept constant in all fits and therefore does not impact on comparison of SF_w values between the different triggers. Certain parameters, which had a tendency towards unphysical values when allowed to be freely fitted, were iterated through in a stepwise manner and the values chosen when the fit was good, both visually and based on the minimum in χ^2 . Uncertainties were taken based on where the fit began to deviate from a visually good quality fit. The best fits for the samples using the 6 different triggers in the 2 mm cuvettes are shown with the data in Fig. S5. All parameters for those fits, including the 5 mm thickness samples, and their uncertainties are provided in Table S2.

	Acetic anhydride	Maleic anhydride	Glutaric anhydride	Diglycolic anhydride	Diglycolic anhydride (5 mm)	GdL	GdL (5 mm)	DCI
Power law scale ($/10^{-5}$)	2 \pm 1	0.8 \pm 0.1	1.9 \pm 0.5	0.9 \pm 0.1	1.6 \pm 0.3	2.1 \pm 0.1	3 \pm 5	1 \pm 1
Power law value, N	2.7 \pm 0.1	3.0 \pm 0.2	2.7 \pm 0.1	3.0 \pm 0.2	2.8 \pm 0.1	2.7 \pm 0.1	2.7 \pm 0.1	3.0 \pm 0.2
Chain scale ($/10^{-3}$)	0.77 \pm 0.01	1.1 \pm 0.2	0.9 \pm 0.1	1.2 \pm 0.1	1.3 \pm 0.2	1.0 \pm 0.2	1.1 \pm 0.1	1.4 \pm 0.2
Radius (nm)	4.4 \pm 1.0	5.5 \pm 1.0	4.4 \pm 1.0	6.0 \pm 1.0	4.4 \pm 1.0	4.4 \pm 1.5	4.4 \pm 0.5	6.0 \pm 1.5
Polydispersity on radius	0.28 \pm 0.2	0.48 \pm 0.2	0.32 \pm 0.25	0.39 \pm 0.04	0.46 \pm 0.1	0.18 \pm 0.08	-	0.35 \pm 0.2
Kuhn length (nm)	14 \pm 5	14 \pm 8	13 \pm 9	22 \pm 8	18 \pm 6	13 \pm 6	12 \pm 7	19 \pm 8
Length (nm)	50 \pm 15	98 \pm 20	54 \pm 15	87 \pm 15	74 \pm 30	52 \pm 15	74 \pm 25	100 \pm 50
Background ($/10^{-3} \text{ cm}^{-1}$)	0.2 \pm 0.2	0.022 \pm 0.005	3.6 \pm 0.2	2.0 \pm 0.5	2.3 \pm 0.2	4.6 \pm 0.1	6 \pm 1	0.5 \pm 0.2

Table S2. The model fit parameters generated by fitting the flexible cylinder model to the data in SasView. Uncertainties were estimated by fixing certain key parameters as described in the text below. Path lengths were 2mm except where otherwise stated.

The greatest uncertainties are on the parameters relating to the longer length scales describing the features of the network and the power law exponent, N (Table S2). This is primarily because of a lack of data at the lowest Q range ($<0.01 \text{ \AA}^{-1}$), which would define these parameters.⁵ Therefore very few conclusions can be drawn from them, the ranges offered by the uncertainties have little impact on the quality of the fit. Here the Kuhn length was left as a variable, based on the assumption that if the radius of the cylinders varies slightly from sample to sample the flexibility may also vary. However, if the Kuhn length were to be kept constant (for example at 15 nm), as one would assume in the analogous field of polymer chains, there is only a very small reduction in the quality of the fit. There are some changes in other correlated parameters (for example length), but the differences are less than the uncertainties already quoted. The radius polydispersity also has a large uncertainty but it is necessary to include this parameter as shown in Fig. S6 which compares the model fit for the GdL sample without the polydispersity parameter alongside the best fit obtained with it.

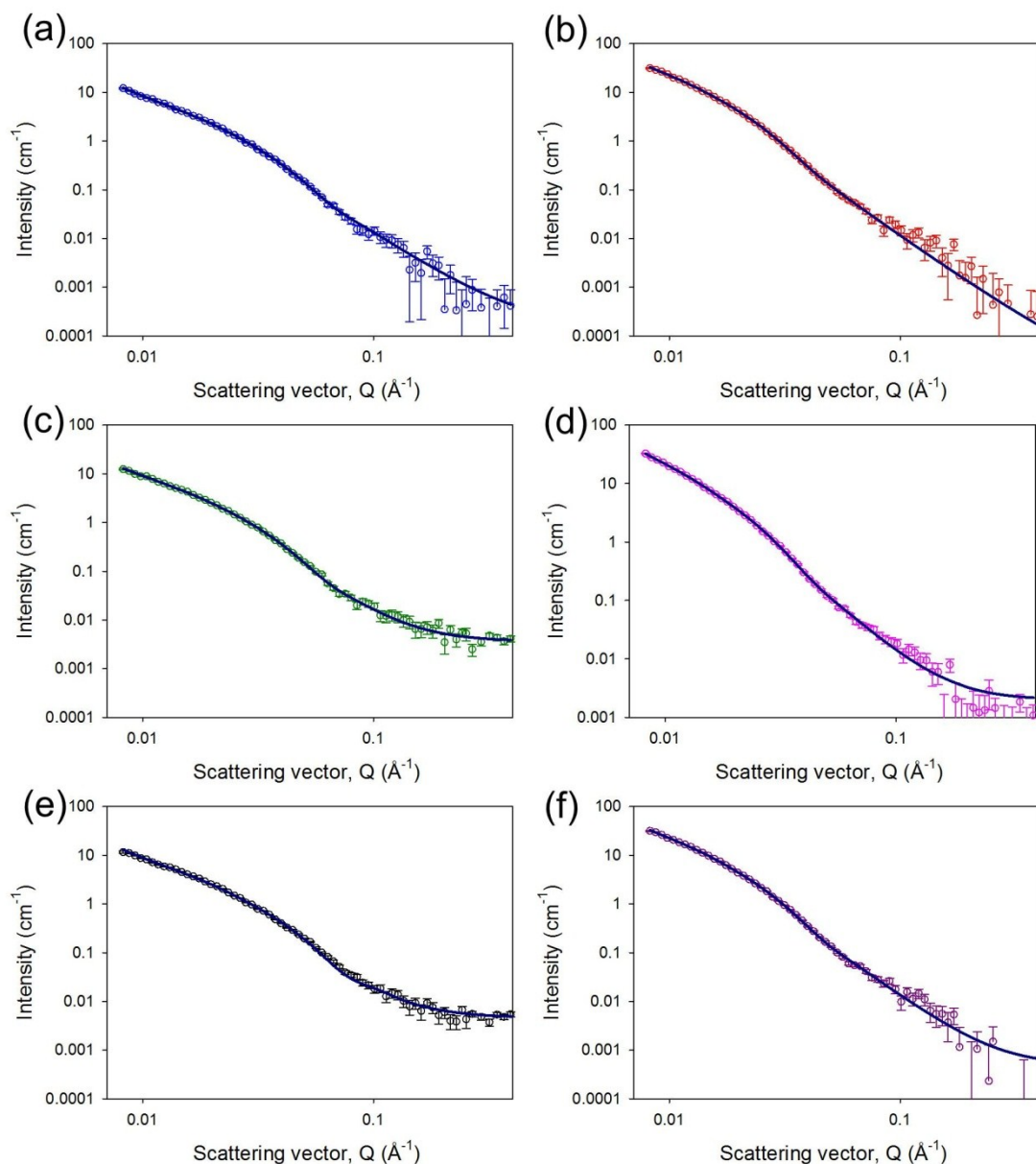


Figure S8. SANS intensity profiles for gels formed using different pH switches (3 molar equivalents with respect to **1**) formed in 2 mm quartz cuvettes. Solid lines represent the model fit generated by the flexible cylinder model described by the parameters given in the following tables. (a) is using acetic anhydride, (b) is using maleic anhydride, (c) is using glutaric anhydride, (d) is using diglycolic anhydride, (e) is using GdL and (f) is using DCI.

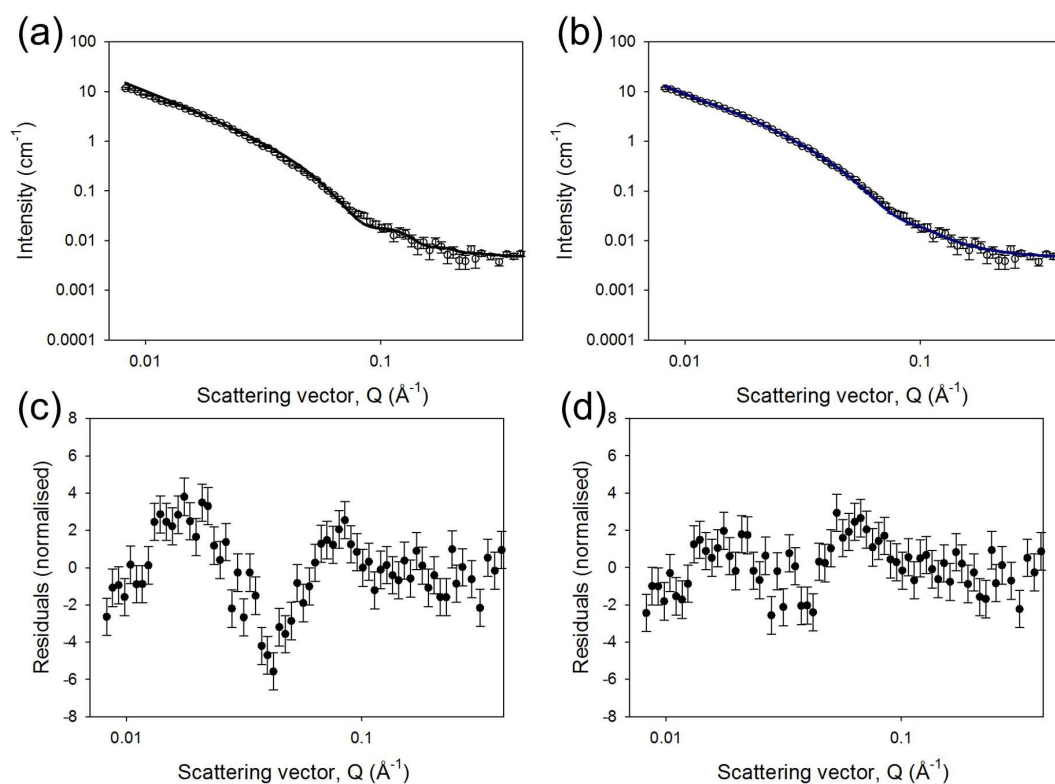


Figure S9. SANS intensity profiles for a gel formed using GdL (3 molar equivalents with respect to **1**) formed in 2 mm quartz cuvettes. Solid lines represent the model fit generated by the flexible cylinder model, (a) without any polydispersity and (b) the best fit with a polydispersity of 0.18. The normalised residuals for each are shown in (c) and (d) respectively.

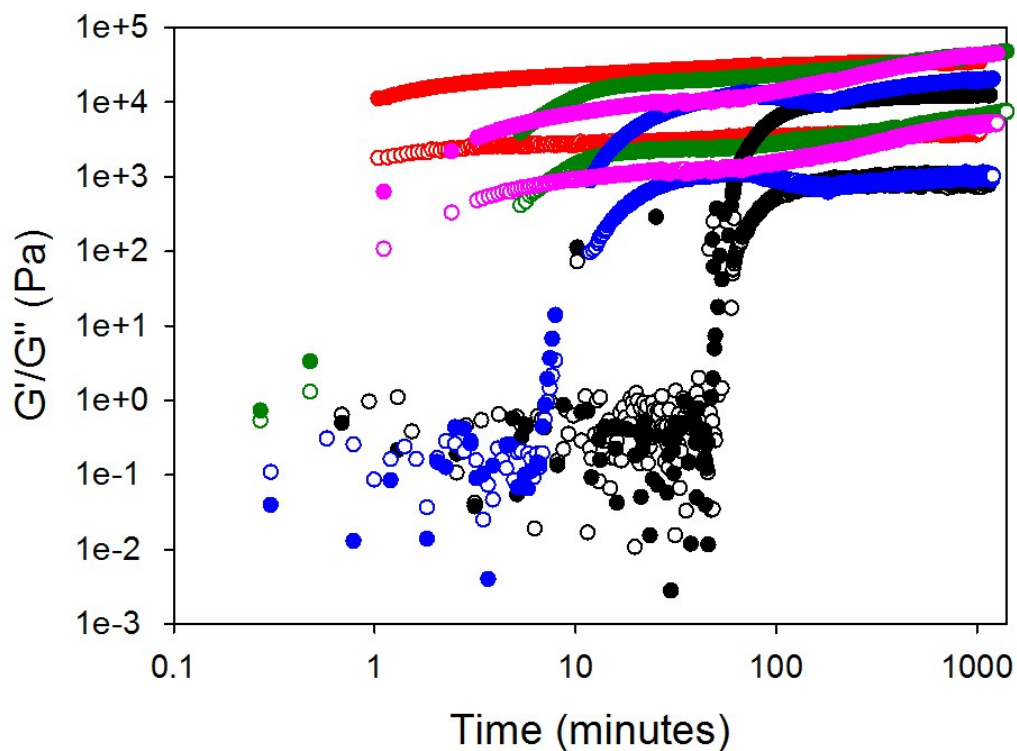


Figure S10. Monitoring gelation of **1** over time at 25 °C (3 molar equivalents of trigger added with respect to **1**). Blue is acetic anhydride, red is maleic anhydride, glutaric anhydride is green, diglycolic anhydride is pink and GdL is black. Full circles represent G' and open circles represent G'' . Measurements were recorded at a strain of 0.5 % and at a frequency of 10 rad/s.

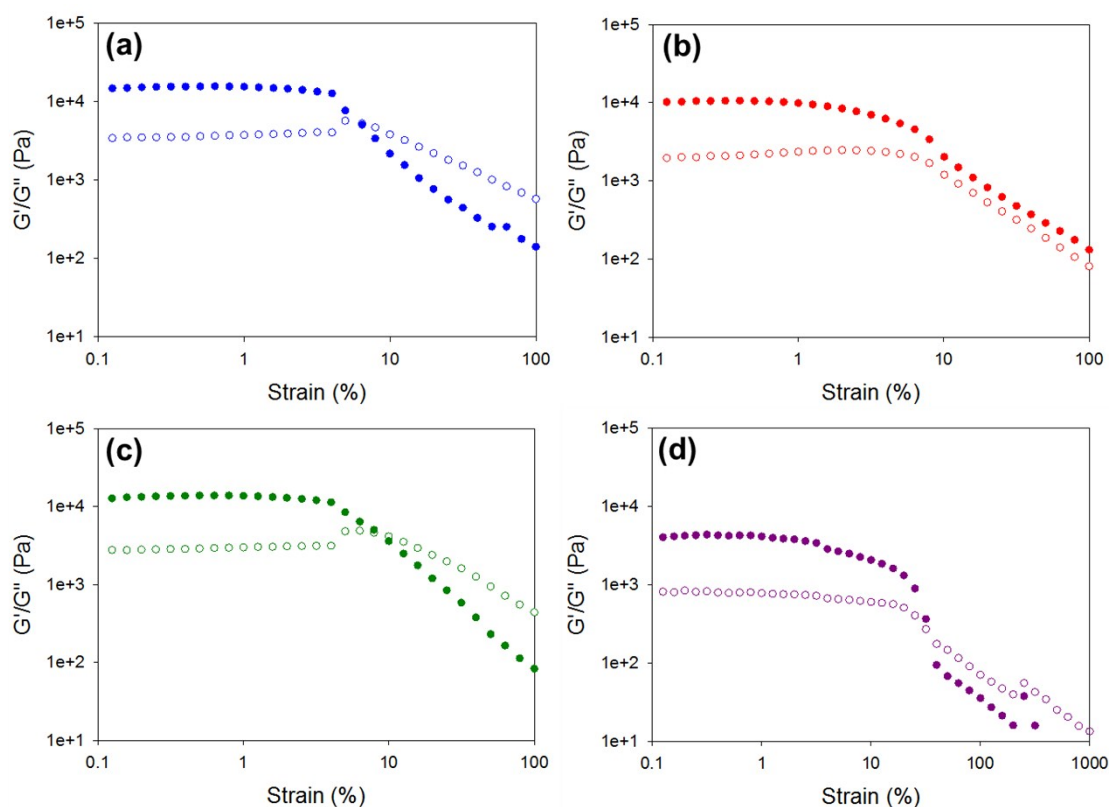


Figure S11. Strain sweeps of gels formed from **1** from 0.1 – 100 % strain using different pH switches (3 molar equivalents of trigger added with respect to **1**). (a) is acetic anhydride, (b) is maleic anhydride, (c) is glutaric anhydride and (d) is HCl. Full circles represent G' and open circles represent G'' . Measurements were performed at a frequency of 10 rad/s at 25 °C.

Molar equivs	Acetic Anhydride	Maleic Anhydride	Glutaric Anhydride	Diglycolic Anhydride	GdL	HCl
1	0.17	0.25	0.17	0.23	0.17	0.17
3	0.23	0.22	0.21	0.21	0.23	0.16
5	0.22	0.20	0.23	0.21	0.22	0.24

Table S4. $\tan \delta$ (data measured by rheology) for gels formed using the different triggers at different molar equivalents with respect to **1**.

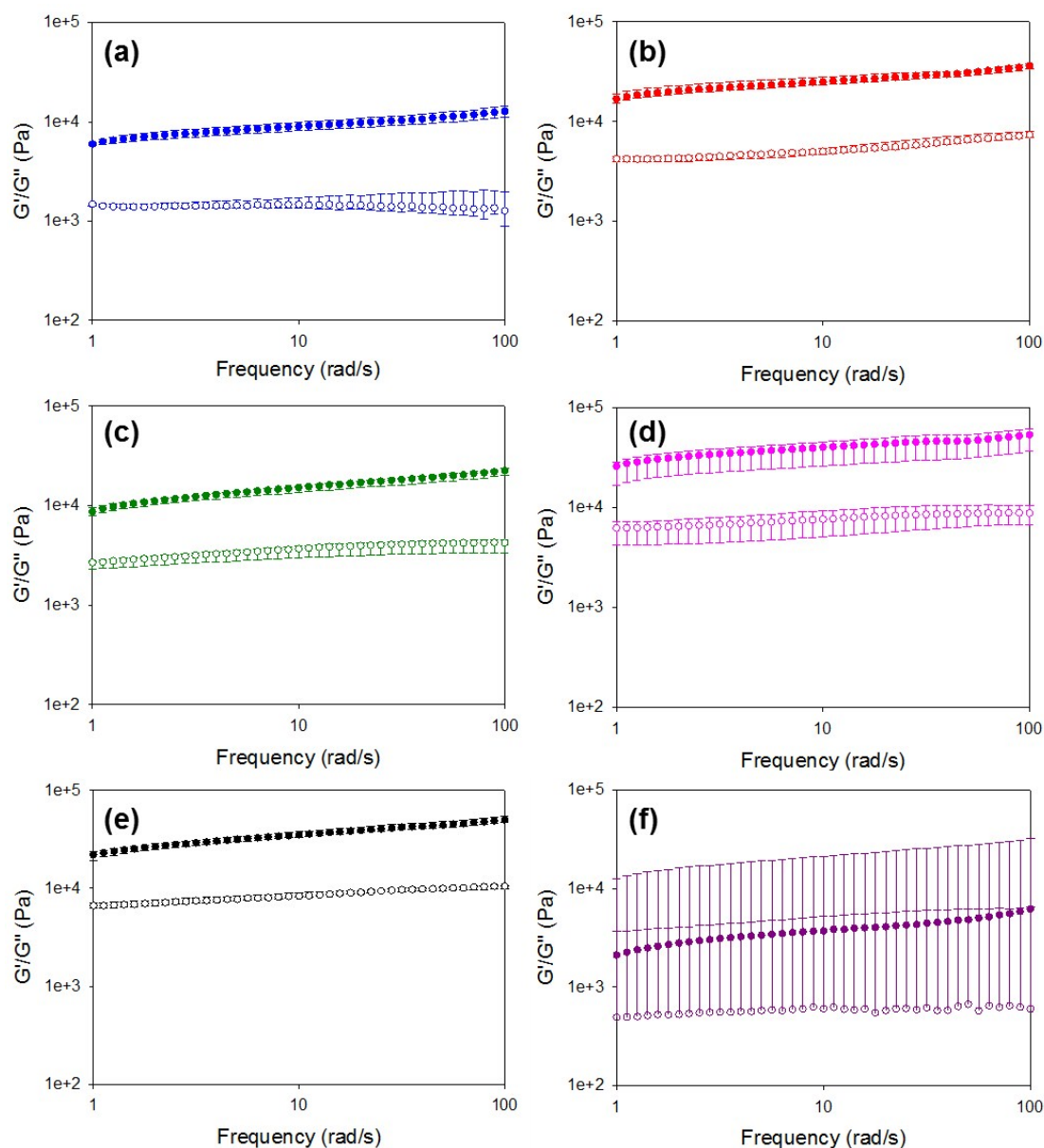


Figure S12. Frequency sweeps from 1 – 100 rad/s with error bars. Error calculated from 3 repeat measurements. For gels formed using different pH switches (3 molar equivalents of trigger added with respect to **1**). Full circles represent G' and open circles represent G'' . (a) is using acetic anhydride, (b) is using maleic anhydride, (c) is using glutaric anhydride, (d) is using diglycolic anhydride, (e) is using GdL and (f) is using HCl. Measurements were performed at 0.5 % strain at 25 °C.

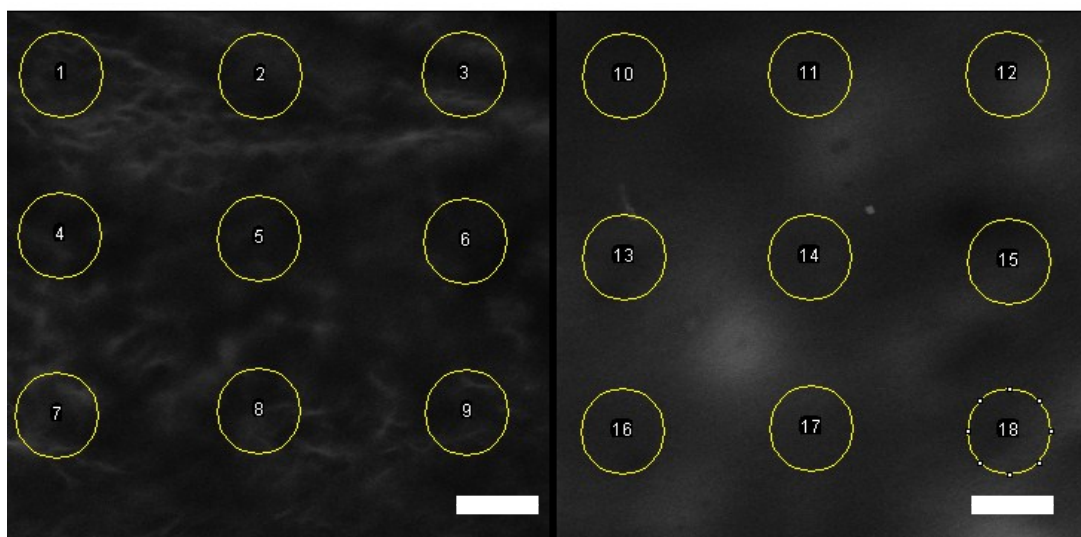


Figure S13. Representative confocal fluorescence microscopy images of gels of **1** triggered using (left) maleic anhydride; (right) acetic anhydride (3 molar equivalents of trigger added with respect to **1**). The circles indicate the size of the indenter tip (100 μm) and the spacing between indents (200 μm). The images indicate how sample heterogeneity is likely to have influenced the variation between the mechanical properties measured at different locations. In both cases, the scale bar is 100 μm . Note that for each gel sample, a 4 x 4 array of indents were carried out with nanoindentation. For clarity, a representative area of 3x3 is shown in this Figure.

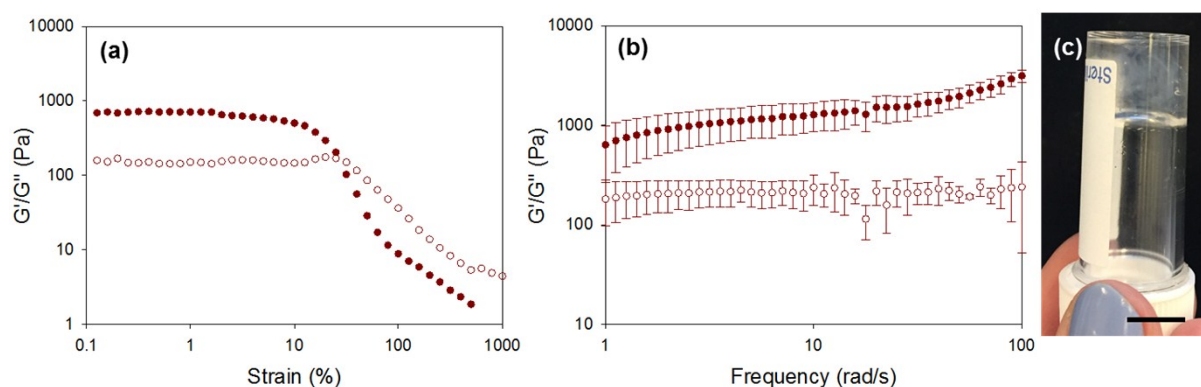


Figure S14. Data for gels formed by the addition of 2 molar equivalents of acetic acid as compared to **1**. (a) strain sweep (b) frequency sweep with error from three measurements (c) is a photograph of gel formed with acetic acid (scale = 1 cm) Strain sweeps performed at 10 rad/s, frequency at 0.5 % strain, all at 25 $^{\circ}\text{C}$.

References

1. www.sasview.org

2. J. S. Pedersen and P. Schurtenberger, *Macromolecules*, **1996**, *29*, 7602-7612.
3. W.-R. Chen, P. D. Butler and L. J. Magid, *Langmuir*, **2006**, *22*, 6539-6548.
4. K. L. Morris, L. Chen, J. Raeburn, O. R. Sellick, P. Cotanda, A. Paul, P. C. Griffiths, S. M. King, R. K. O'Reilly, L. C. Serpell and D. J. Adams, *Nat. Commun.*, **2013**, *4*, 1480.
5. R. A. Hule, R. P. Nagarkar, A. Altunbas, H. R. Ramay, M. C. Branco, J. P. Schneider and D. J. Pochan, *Faraday Discuss.*, **2008**, *139*, 251-264.